NANO LETTERS

2005
Vol. 5, No. 2
269−274

Kelvin Probe Force Microscopy Study on Conjugated Polymer/Fullerene Bulk Heterojunction Organic Solar Cells

H. Hoppe,*,† T. Glatzel,‡ M. Niggemann,§ A. Hinsch,§ M. Ch. Lux-Steiner,‡ and N. S. Sariciftci†

Linz Institute for Organic Solar Cells (LIOS), Physical Chemistry, Johannes Kepler University Linz, Altenbergerstr. 69, A-4040 Linz, Austria, Hahn-Meitner Institut, Glienicker Strasse 100, 14109 Berlin, Germany, and Fraunhofer Institute for Solar Energy Systems (ISE), Heidenhofstr. 2, D-79110 Freiburg, Germany

Received November 3, 2004; Revised Manuscript Received November 26, 2004

ABSTRACT

We conducted a comprehensive Kelvin probe force microscopy (KPFM) study on a classical organic solar cell system consisting of MDMO–PPV/PCBM blends. The KPFM method yields the information of topography and local work function at the nanometer scale. Experiments were performed either in the dark or under cw laser illumination at 442 nm. We identified distinct differences in the energetics on the surface of chlorobenzene and toluene cast blend films. Together with high-resolution scanning electron microscopy (SEM) experiments we were able to interpret the KPFM results and to draw some conclusions for the electron transport toward the cathode in the solar cell configuration. The results suggest that surfaces of toluene cast films exhibit a morphologically controlled hindrance for electron propagation toward the cathode, which is usually evaporated on top of the films in the solar cell device configuration.

Organic solar cells have become a subject of increasing research interest within the past few years.[1−8] Dominant configurations are either bilayer heterojunctions[9−15] or bulk heterojunctions.[7,16−19] Whereas the bilayer heterojunctions have been fabricated with comparably high efficiencies using small organic molecules,[13] a breakthrough in power conversion efficiency in polymer solar cells was achieved for bulk heterojunctions with the MDMO−PPV/PCBM (poly-[2-(3,7-dimethyloctyloxy)-5-methyloxy]-para-phenylene-vinylene/1-(3-methoxycarbonyl) propyl-1-phenyl [6,6]C61) system.[20] The drastic increase in the power conversion efficiency was a result of changing the spin casting solvent from toluene to chlorobenzene, which accounted for a change in the film nanomorphology.[20] More detailed studies on this system revealed a finer intermixing of the polymer and fullerene constituents when spin cast from chlorobenzene solution.[21−23] Since the charge separation in bulk heterojunctions is based on the photoinduced charge transfer,[24] and photoexcited excitons in organic materials have a very limited diffusion length on the order of 10 nm,[11,25−28] it is evident that for coarse-grained morphologies with characteristic domain sizes above 50 nm, not all photoexcitations will dissociate into separated charge carriers. Indeed a relatively strong photoluminescence of PCBM was found for toluene cast blends,[23] which could be detected locally by near-field scanning optical microscopy.[29] This means that part of the absorbed photons is not used for photocurrent generation. Another study reported the hole mobility of pristine MDMO−PPV films to decrease when cast from toluene as compared to chlorobenzene.[30] These differences in mobility as well as the limits in charge generation have been used to model the observed device behavior.[31] Here we report KPFM results on MDMO−PPV/PCBM films, which show clear differences in the electronic work functions for the different morphologies observed, indicating the lower photocurrent of toluene cast samples to be also due to hindered electron transport toward the cathode.

All pristine and mixed solutions of MDMO−PPV and PCBM were stirred overnight under slightly elevated (50 °C) temperatures, without any sonication or filtering. Solution concentrations were 3, 0.25, and 1.25 wt % for PCBM, MDMO−PPV, and MDMO−PPV/PCBM 1:4 blends, respectively. Films were produced by spin casting at 1500 rpm onto precleaned ITO glass, resulting in a thickness of typically 50−100 nm. All steps in the production of the films were performed inside an argon glovebox in order to prevent any oxygen or water contamination. All samples were sealed inside the glovebox for the transport. Again under argon atmosphere the samples were loaded into the magazine of

* Corresponding author. E-mail: harald.hoppe@jku.at.
† Johannes Kepler University Linz.
‡ Hahn-Meitner Institut.
§ Fraunhofer Institute for Solar Energy Systems.

10.1021/nl048176c CCC: $30.25
Published on Web 01/12/2005

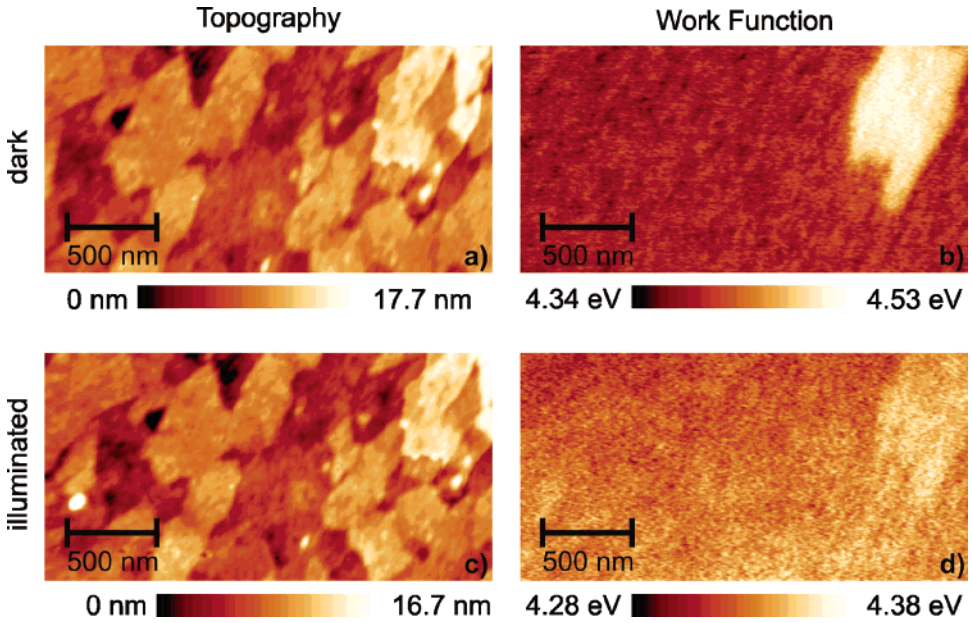

Figure 1. Topography (a, c) and work function (b, d) of a pristine MDMO−PPV film in the dark (a, b) and under 442 nm HeCd laser illumination (c, d).

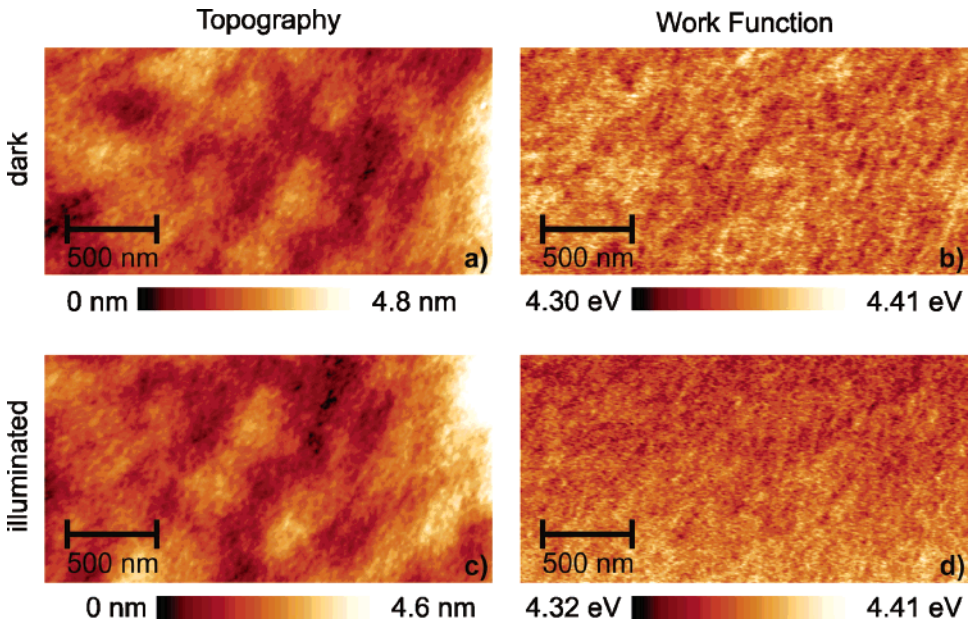

Figure 2. Topography (a, c) and work function (b, d) of a pristine PCBM film in the dark (a, b) and under 442 nm HeCd laser illumination (c, d).

the KPFM and transferred into the vacuum system (pressure $p < 10^{-10}$ mbar) without allowing any air to enter.

The application of scanning probe microscopes (SPMs) has increased the understanding of the physics of surfaces on the nanometer scale, even down to the atomic level.[32,33] Most SPMs are based on the atomic force microscope, which uses a sharp tip at the end of a cantilever to sense the attractive and/or repulsive forces while scanning over a sample surface. The Kelvin probe force microscope (KPFM) measures the height variations on the sample surface and, simultaneously, employs the electrostatic forces between sample and tip that, finally, yield the contact potential (CP).[34−36] Once the work function Φ_{tip} of the cantilever is known, it is possible to determine the work function Φ_{sample} of the sample from the measured CP according to $\Phi_{sample} = \Phi_{tip} + q\mathrm{CP}$, where q is the elementary charge. For a quantitative study of the work function, samples have to be kept under ultrahigh vacuum (UHV) conditions, since adsorbates strongly alter the work function of a surface.[37,38] For the study of semiconductors and organic materials, the KPFM has recently become an important tool. It is now possible to unravel lateral inhomogeneities of surfaces, also in technologically relevant devices.[39,40] In addition, the study of material parameters such as the diffusion length[41] and the influence of surface states and single charges at the Fermi level position at the surface[42,43] have become possible on a nanometer scale. KPFM has already been applied earlier to

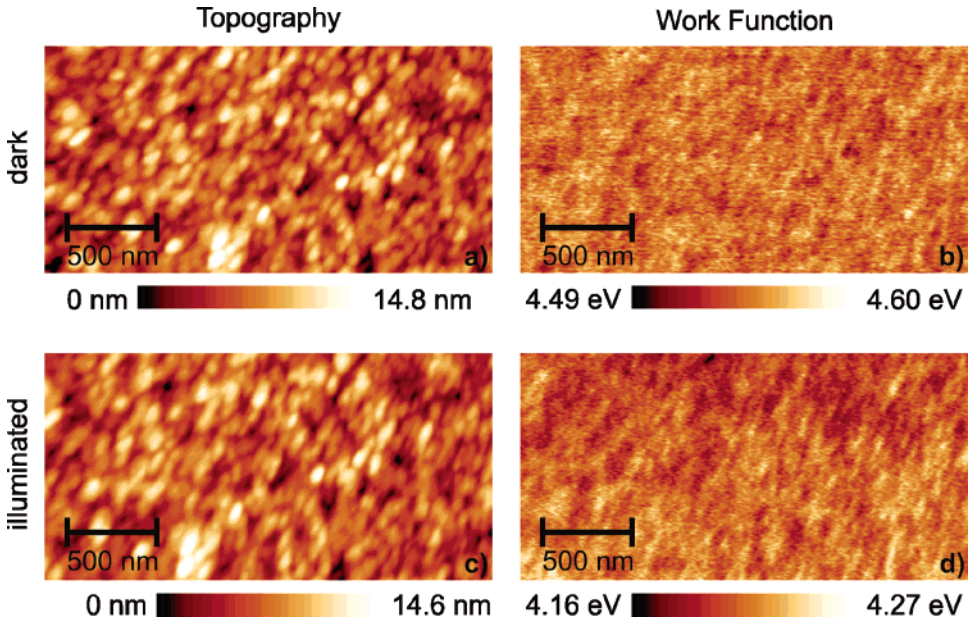

Figure 3. Topography (a, c) and work function (b, d) of a chlorobenzene-cast blend film of MDMO−PPV/PCBM with a mass ratio of 1:4, measured in the dark (a, b) and under 442 nm cw laser illumination (c, d).

organic films[44] and for mapping of the electric potential across thin film organic field effect transistors.[45−47]

The UHV−KPFM measurements take place in a modified Omicron UHV−STM/AFM (at a pressure $p < 10^{-10}$ mbar). The topography is determined using the standard frequency modulation technique at the first resonance frequency of the cantilever (about 70 kHz[48]). Amplitude modulation detection at the cantilever's second resonance frequency with an ac-bias amplitude as small as 100 mV_{pp} facilitates simultaneous imaging of the CP, which is compensated by applying the corresponding voltage to the sample.[36,49] See ref 48 for further details on the UHV−KPFM. For all measurements, PtIr-coated Si cantilevers ($\Phi = 4.28 \pm 0.07$ eV) are used. To determine the surface photovoltage (SPV) of the samples, i.e., the change of the work function with illumination, the sample is illuminated with a HeCd laser (wavelength $\lambda =$ 442 nm). All other measurements are performed under dark conditions.

Scanning electron microscopy (SEM) measurements were performed using a cold field emission scanning electron microscope (Hitachi S-4700). Prior to imaging, the samples were covered by sputtering a thin platinum layer on their broken edge or on their top.

ITO-covered glass was purchased from Merck (Darmstadt, Germany). MDMO−PPV (poly-[2-(3,7-dimethyloctyloxy)-5-methyloxy]-para-phenylene-vinylene) was provided by Covion (Frankfurt, Germany). PCBM (1-(3-methoxycarbonyl) propyl-1-phenyl [6,6]C_{61}) was purchased from J. C. Hummelen (University of Groningen, The Netherlands).

At first we used the KPFM to investigate the pristine materials, both under cw-laser illumination and in the dark. In Figure 1, the topography and the local work function are shown for an MDMO−PPV film spin cast on ITO. Interestingly, the topography of the pristine MDMO−PPV film (Figure 1a,c) exhibits the same features as for ITO alone (structure of platelets). However, the work function is mostly unaffected by the platelet structure and an average value of 4.4 eV is found (Figure 1b,d). Under illumination there is a shift of the work function toward slightly smaller values, yielding an average value closer to 4.3 eV.

In the case of pristine PCBM (compare Figure 2) we find a more homogeneous and smoother surface topography than for MDMO−PPV as a result of a higher film thickness (Figure 2a,c). Also here, the work function does not vary much and it is centered between 4.3 and 4.4 eV in the dark (Figure 2b) and very similarly under illumination (Figure 2d).

Figure 3 displays the measurements obtained on the blend film of MDMO−PPV and PCBM spin cast from chlorobenzene, both under light and in the dark. The average value of the work function in the dark is between 4.5 and 4.6 eV. Upon illumination the work function is shifted strongly down to 4.2 eV.

For toluene-cast MDMO−PPV/PCBM blends, the situation is different (compare Figure 4). First there is a broader range of values of the work function, depending on the place on the sample. In the dark the work function ranges between 4.4 and 4.6 eV, whereas under illumination the spread is almost doubled and the highest work functions detected are about 4.7 eV.

In general, we observe a larger work function on top of the elevations caused by the PCBM clusters (compare[23]). Shifting to a larger work function corresponds to a reduction of electron and respectively an increase of hole density. Hence the top layer above the PCBM clusters should be enriched with holes as compared to the pristine films or the blend in the dark.

While for the blend cast from chlorobenzene (Figure 3) the work function in the dark has similar high or larger values (∼4.55 eV) as the work function of the toluene cast blend, the situation under illumination is reversed. In the case of chlorobenzene-cast blend films the work function shifts

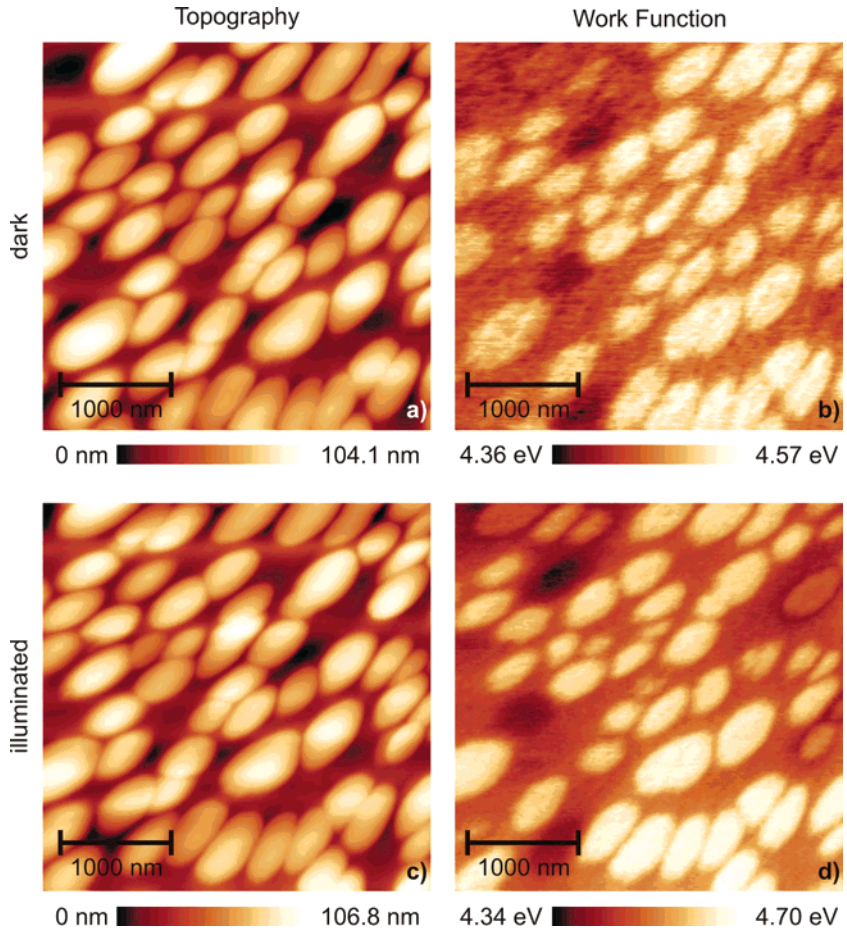

Figure 4. Topography and work function of a toluene-cast blend film of MDMO−PPV/PCBM with a mass ratio of 1:4, measured in the dark and under 442 nm cw laser illumination. Note that some of the topographical hills lead to dark areas and thus low work functions, whereas the majority of the hills result in bright areas with high work functions.

toward lower values around 4.2 eV, whereas the lowest values on toluene-cast blend films are roughly 4.3 eV. Medium values of about 4.4 eV are generally found between the elevations of PCBM clusters, whereas on top of these clusters the work function is generally increased up to 4.7 eV (compare Figure 4).

From SEM measurements it follows that polymeric nanospheres are generally located on top of the PCBM clusters, as demonstrated recently.[23] On the other hand the blend films cast from chlorobenzene expose both the polymer and the fullerene phases toward the surface of the film. This can be clearly seen in Figure 5, where chlorobenzene- and toluene-cast blends are compared with each other. Here the polymer nanospheres are distributed almost evenly throughout the bulk of the film, whereas a so-called skin layer, incorporating polymer nanospheres, surrounds the big PCBM clusters in toluene cast films.

However, in Figure 4 there are some remarkable exceptions: on top of some PCBM elevations, a minimum value of ∼4.3 eV is obtained for the work function. Also, Martens et al.[46] reported a similar behavior for a single KPFM measurement on a particular PCBM cluster. This again can be understood with the help of high-resolution SEM measurements: in some cases the PCBM clusters are not covered by polymer nanospheres, but they are exposed freely to the film surface. Some examples of that are shown in Figure 6 for illustration.

Since according to the photoinduced charge transfer[24] we expect the highest electron concentration within the pure PCBM phase, it is obvious that the extraction of electrons from these locations is energetically much more easy than extraction through a hole-enriched polymer barrier layer. Therefore, the increased contrast in work function on the illuminated toluene blend reflects the increase in local concentrations of holes and electrons due to the photoinduced charge transfer. As a result, the skin layer around the PCBM clusters in the toluene-cast blends may cause a severe limitation for electron transport toward the cathode due to insufficient percolation and recombination. As a conclusion and in addition to an incomplete charge transfer due to too small exciton diffusion lengths in these largely phase separated structures, this barrier will be another reason for the smaller photocurrents and thus power conversion efficiencies observed in toluene-cast blends. Furthermore, some of the freely exposed PCBM nanoclusters should result in "hot spots" with a locally larger photocurrent generation. It should be possible to measure this directly by the recently presented NSOM-based local photocurrent mapping technique.[50] On the other hand, the reduced work function on

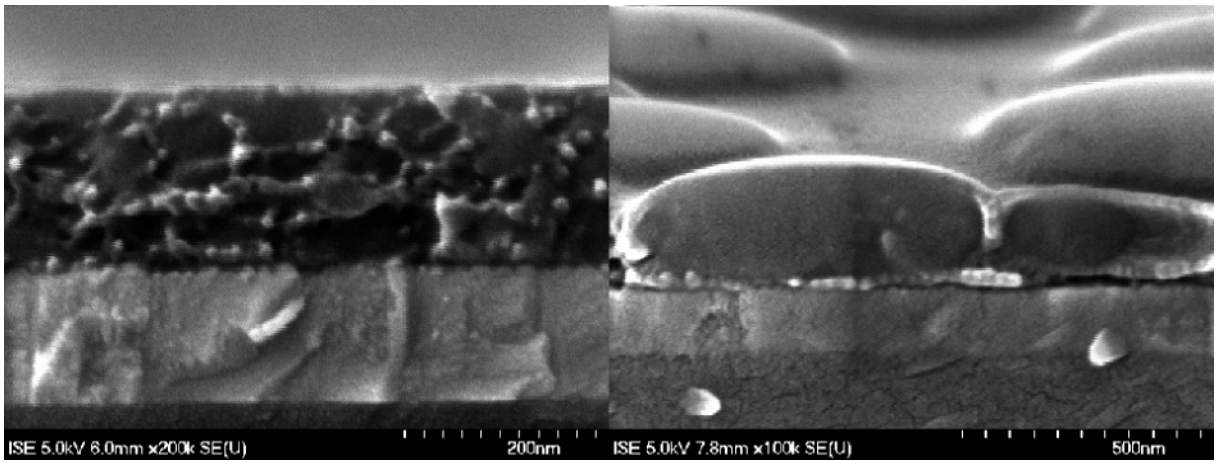

Figure 5. SEM measurements on cross sections of MDMO−PPV/PCBM 1:4 blends. On the left a chlorobenzene- and on the right a toluene-cast film are shown for comparison. Polymer nanospheres (brighter) are rather evenly distributed in the film on the left, while they surround the large PCBM clusters as a "skin-layer" in the right.[23]

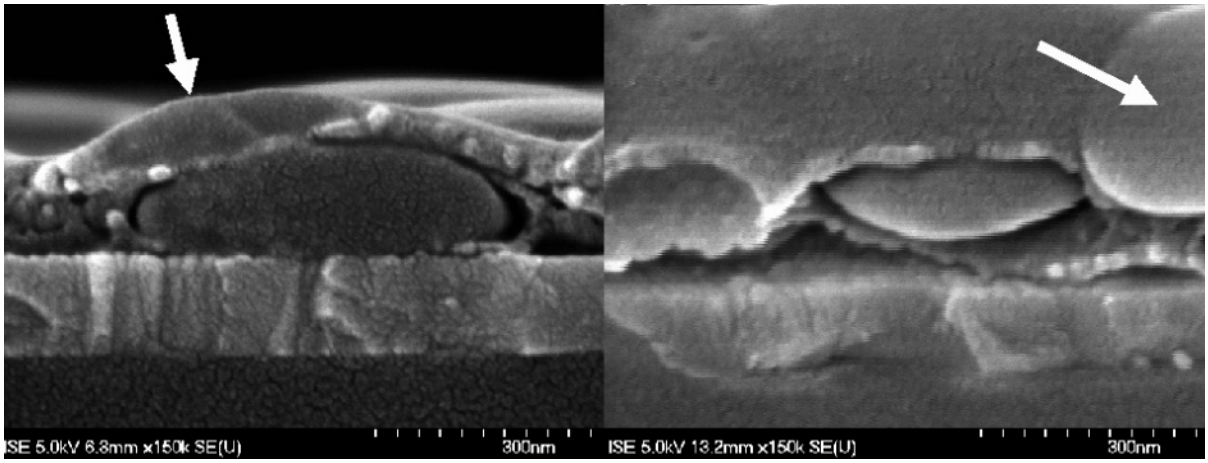

Figure 6. Cross-sectional SEM images of toluene-cast MDMO−PPV/PCBM blend films. The white arrows point to regions where PCBM clusters are exposed freely to the surface of the film.

illuminated chlorobenzene cast blends reflects a favorable increase of the electron concentration at the film surface.

In conclusion, we demonstrated Kelvin probe force microscopy to be a powerful tool for the investigation of organic solar cells. In connection with high-resolution scanning electron measurements, we were able to identify a barrier for electron transmission from the electron-rich PCBM nanoclusters toward the extracting cathode. This depicts an additional reason for the spectrally independent smaller photocurrents and lower power conversion efficiencies of toluene-cast MDMO−PPV/PCBM blends as compared to chlorobenzene-cast blends, which once again is related strongly to the nanomorphology in the bulk heterojunction. Hence not only the exciton diffusion and the appropriate size of phase separation are important for efficient organic solar cells, but also the connectivity and percolation of both the electron and hole transporting phases with their respective electrodes appear to be a major factor.

Acknowledgment. Part of this work was performed within the Christian Doppler Society's dedicated laboratory on Plastic Solar Cells co-funded by Konarka Corporation. Part of this work was financed with the help of the German Ministry for Education and Research (BMBF, contract numbers 01SF0026 and 01SF0119).

References

(1) Brabec, C. J.; Sariciftci, N. S.; Hummelen, J. C. *Adv. Funct. Mater.* **2001**, *11*, 15.
(2) Halls, J. J. M.; Friend, R. H. In *Clean Electricity from Photovoltaics*; Archer, M. D., Hill, R., Eds.; Imperial College Press: London, 2001.
(3) Nelson, J. *Curr. Opin. Solid State Mater. Sci.* **2002**, *6*, 87.
(4) Nunzi, J.-M. *C. R. Phys.* **2002**, *3*, 523.
(5) *Organic Photovoltaics: Concepts and Realization*; Brabec, C. J., Dyakonov, V., Parisi, J., Sariciftci, N. S., Eds.; Springer: Berlin, 2003; Vol. 60.
(6) Peumans, P.; Yakimov, A.; Forrest, S. R. *J. Appl. Phys.* **2003**, *93*, 3693.
(7) Maennig, B.; Drechsel, J.; Gebeyehu, D.; Simon, P.; Kozlowski, F.; Werner, A.; Li, F.; Grundmann, S.; Sonntag, S.; Koch, M.; Leo, K.; Pfeiffer, M.; Hoppe, H.; Meissner, D.; Sariciftci, N. S.; Riedel, I.; Dyakonov, V.; Parisi, J. *Appl. Phys. A* **2004**, *79*, 1.
(8) Hoppe, H.; Sariciftci, N. S. *J. Mater. Res.* **2004**, *19*, 1924.
(9) Tang, C. W. *Appl. Phys. Lett.* **1986**, *48*, 183.
(10) Sariciftci, N. S.; Braun, D.; Zhang, C.; Srdanov, V. I.; Heeger, A. J.; Stucky, G.; Wudl, F. *Appl. Phys. Lett.* **1993**, *62*, 585.
(11) Pettersson, L. A. A.; Roman, L. S.; Inganäs, O. *J. Appl. Phys.* **1999**, *86*, 487.
(12) Peumanns, P.; Bulovic, V.; Forrest, S. R. *Appl. Phys. Lett.* **2000**, *76*, 2650.
(13) Peumanns, P.; Forrest, S. R. *Appl. Phys. Lett.* **2001**, *79*, 126.

(14) Peumans, P.; Forrest, S. R. Erratum: [*Appl. Phys. Lett.* **2001**, *79*, 126], *Appl. Phys. Lett.* **2002**, *80*, 338.
(15) Rostalski, J.; Meissner, D. *Sol. Energy Mater. Sol. Cells* **2000**, *63*, 37.
(16) Yu, G.; Gao, J.; Hummelen, J. C.; Wudl, F.; Heeger, A. J. *Science* **1995**, *270*, 1789.
(17) Halls, J. J. M.; Walsh, C. A.; Greenham, N. C.; Marseglia, E. A.; Friend, R. H.; Moratti, S. C.; Holmes, A. B. *Nature* **1995**, *376*, 498.
(18) Tada, K.; Hosada, K.; Hirohata, M.; Hidayat, R.; Kawai, T.; Onoda, M.; Teraguchi, M.; Masuda, T.; Zakhidov, A. A.; Yoshino, K. *Synth. Met.* **1997**, *85*, 1305.
(19) Hiramoto, M.; Fujiwara, H.; Yokoyama, M. *Appl. Phys. Lett.* **1991**, *58*, 1062.
(20) Shaheen, S. E.; Brabec, C. J.; Sariciftci, N. S.; Padinger, F.; Fromherz, T.; Hummelen, J. C. *Appl. Phys. Lett.* **2001**, *78*, 841.
(21) Martens, T.; D'Haen, J.; Munters, T.; Beelen, Z.; Goris, L.; Manca, J.; D'Olieslaeger, M.; Vanderzande, D.; Schepper, L. D.; Andriessen, R. *Synth. Met.* **2003**, *138*, 243.
(22) Yang, X.; van Duren, J. K. J.; Janssen, R. A. J.; Michels, M. A. J.; Loos, J. *Macromolecules* **2004**, *37*, 2151.
(23) Hoppe, H.; Niggemann, M.; Winder, C.; Kraut, J.; Hiesgen, R.; Hinsch, A.; Meissner, D.; Sariciftci, N. S. *Adv. Funct. Mater.* **2004**, *14*, 1005.
(24) Sariciftci, N. S.; Smilowitz, L.; Heeger, A. J.; Wudl, F. *Science* **1992**, *258*, 1474.
(25) Halls, J. J. M.; Pichler, K.; Friend, R. H.; Moratti, S. C.; Holmes, A. B. *Appl. Phys. Lett.* **1996**, *68*, 3120.
(26) Haugeneder, A.; Neges, M.; Kallinger, C.; Spirkl, W.; Lemmer, U.; Feldmann, J.; Scherf, U.; Harth, E.; Gügel, A.; Müllen, K. *Phys. Rev. B* **1999**, *59*, 15346.
(27) Stübinger, T.; Brütting, W. *J. Appl. Phys.* **2001**, *90*, 3632.
(28) Kroeze, J. E.; Savanije, T. J.; Vermeulen, M. J. W.; Warman, J. M. *J. Phys. Chem. B* **2003**, *107*, 7696.
(29) Röder, T.; Kitzerow, H.-S.; Hummelen, J. C. *Synth. Met.* **2004**, *141*, 271.
(30) Geens, W.; Shaheen, S. E.; Wessling, B.; Brabec, C. J.; Poortmans, J.; Sariciftci, N. S. *Org. Electron.* **2002**, *3*, 105.
(31) Geens, W.; Martens, T.; Poortmans, J.; Aernouts, T.; Manca, J.; Lutsen, L.; Heremans, P.; Borghs, S.; Mertens, R.; Vanderzande, D. *Thin Solid Films* **2004**, *451*−*452*, 498.
(32) Wiesendanger, R.; *Scanning Probe Microscopy and Spectroscopy: Methods and Applications*; Cambridge University Press: Cambridge, 1994.
(33) Binnig, G.; Rohrer, H. *Rev. Mod. Phys.* **1999**, *71*, S324.
(34) Weaver, J. M. R.; Abraham, D. W. *J. Vac. Sci. Technol. B* **1991**, *9*, 1559.
(35) Kitamura, S.; Iwatsuki, M. *Appl. Phys. Lett.* **1998**, *72*, 3154.
(36) Kikukawa, A.; Hosaka, S.; Imura, R. *Appl. Phys. Lett.* **1995**, *66*, 3510.
(37) Jean, M. S.; Hudlet, S.; Guthmann, C.; Berger, J. *Phys. Rev. B* **1997**, *56*, 15391−15395.
(38) Itoh, J.; Nazuka, Y.; Kanemaru, S.; Inoue, T.; Yokoyama, H.; Shimizu, K. *J. Vac. Sci. Technol. B* **1996**, *14*, 2105.
(39) Tanimoto, M.; Vatel, O. *J. Vac. Sci. Technol. B* **1996**, *14*, 1547.
(40) Glatzel, T.; Marrón, D. F.; Schedel-Niedrig, T.; Sadewasser, S.; Lux-Steiner, M. C. *Appl. Phys. Lett.* **2002**, *81*, 2017.
(41) Shikler, R.; Fried, N.; Meoded, T.; Rosenwaks, Y. *Phys. Rev. B* **2000**, *61*, 11041−11046.
(42) Glatzel, T.; Sadewasser, S.; Shikler, R.; Rosenwaks, Y.; Lux-Steiner, M. C. *Mater. Sci. Eng. B* **2003**, *102*, 138.
(43) Sommerhalter, C.; Matthes, T. W.; Glatzel, T.; Jäger-Waldau, A.; Lux-Steiner, M. C. *Appl. Phys. Lett.* **1999**, *75*, 286.
(44) Yamada, H.; Fukuma, T.; Umeda, K.; Kobayashi, K.; Matsushige, K. *Appl. Surf. Sci.* **2002**, *188*, 391.
(45) Bürgi, L.; Sirringhaus, H.; Friend, R. H. *Appl. Phys. Lett.* **2002**, *80*, 2913.
(46) Martens, T.; Beelen, Z.; D'Haen, J.; Munters, T.; Goris, L.; Manca, J.; D'Olieslaeger, M.; Vanderzande, D.; Schepper, L. D.; Andriessen, R. Morphology of MDMO−PPV:PCBM bulk hetero-junction organic solar cells studied by AFM, KFM and TEM; Kafafi, Z. H., Fichou, D., Eds.; Organic Photovoltaics III; *Proceedings of the SPIE−The International Society for Optical Engineering*, San Diego, CA, 2003; Vol. 4801, p 40.
(47) Nichols, J. A.; Gundlach, D. J.; Jackson, T. N. *Appl. Phys. Lett.* **2003**, *83*, 2366.
(48) Sommerhalter, C.; Glatzel, T.; Matthes, T. W.; Jäger-Waldau, A.; Lux-Steiner, M. C. *Appl. Surf. Sci.* **2000**, *157*, 263.
(49) Glatzel, T.; Sadewasser, S.; Lux-Steiner, M. C. *Appl. Surf. Sci.* **2003**, *210*, 84.
(50) McNeill, C. R.; Frohne, H.; Holdsworth, J. L.; Furst, J. E.; King, B. V.; Dastoor, P. C. *Nano Lett.* **2004**, *4*, 219.

NL048176C